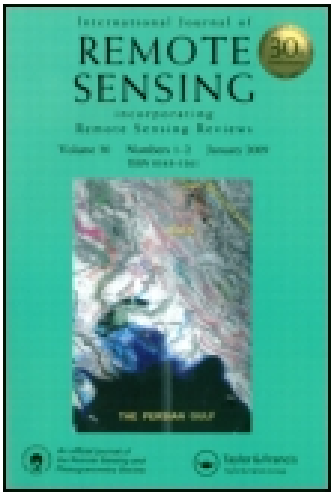

International Journal of Remote Sensing
Publication details, including instructions for authors and subscription information:
http://www.tandfonline.com/loi/tres20

A maximum entropy method to extract urban land by combining MODIS reflectance, MODIS NDVI, and DMSP-OLS data

Jinyao Lin[a], Xiaoping Liu[a], Kai Li[a] & Xia Li[a]
[a] School of Geography and Planning, and Guangdong Key Laboratory for Urbanization and Geo-simulation, Sun Yat-sen University, Guangzhou, Guangdong 510275, PR China
Published online: 17 Oct 2014.

To cite this article: Jinyao Lin, Xiaoping Liu, Kai Li & Xia Li (2014) A maximum entropy method to extract urban land by combining MODIS reflectance, MODIS NDVI, and DMSP-OLS data, International Journal of Remote Sensing, 35:18, 6708-6727, DOI: 10.1080/01431161.2014.960623

To link to this article: http://dx.doi.org/10.1080/01431161.2014.960623

International Journal of Remote Sensing, 2014
Vol. 35, No. 18, 6708–6727, http://dx.doi.org/10.1080/01431161.2014.960623

A maximum entropy method to extract urban land by combining MODIS reflectance, MODIS NDVI, and DMSP-OLS data

Jinyao Lin, Xiaoping Liu*, Kai Li, and Xia Li

School of Geography and Planning, and Guangdong Key Laboratory for Urbanization and Geo-simulation, Sun Yat-sen University, Guangzhou, Guangdong 510275, PR China

(*Received 9 May 2014; accepted 24 July 2014*)

Researchers often encounter difficulties in obtaining timely and detailed information on urban growth. Modern remote-sensing techniques can address such difficulties. With desirable spectral resolution and temporal resolution, Moderate Resolution Imaging Spectroradiometer (MODIS) products have significant advantages in tackling land-use and land-cover change issues at regional and global scales. However, simply based on spectral information, traditional methods of remote-sensing image classification are barely satisfactory. For example, it is quite difficult to distinguish urban and bare lands. Moreover, training samples of all land-cover types are needed, which means that traditional classification methods are inefficient in one-class classification. Even support vector machine, a current state-of-the-art method, still has several drawbacks. To address the aforementioned problems, this study proposes extracting urban land by combining MODIS surface reflectance, MODIS normalized difference vegetation index (NDVI), and Defense Meteorological Satellite Program Operational Linescan System data based on the maximum entropy model (MAXENT). This model has been proved successful in solving one-class problems in many other fields. But the application of MAXENT in remote sensing remains rare. A combination of NDVI and Defense Meteorological Satellite Program Operational Linescan System data can provide more information to facilitate the one-class classification of MODIS images. A multi-temporal case study of China in 2000, 2005, and 2010 shows that this novel method performs effectively. Several validations demonstrate that the urban land extraction results are comparable to classified Landsat TM (Thematic Mapper) images. These results are also more reliable than those of MODIS land-cover type product (MCD12Q1). Thus, this study presents an innovative and practical method to extract urban land at large scale using multiple source data, which can be further applied to other periods and regions.

1. Introduction

As a consequence of rapid urbanization and population growth worldwide, urban land has expanded to an unprecedented size, especially in the developing world (Grimm et al. 2008; Li et al. 2013). Monitoring the spatial extent of urban land has become crucial for researchers (Stefanov, Ramsey, and Christensen 2001; Small, Pozzi, and Elvidge 2005). Although several international groups have developed eight different global urban maps, such as the Global Rural–Urban Mapping Project (Balk et al. 2006), the urban land areas derived from these maps can vary from 0.3 to 3.5 million km^2 (Potere et al. 2009; Schneider, Friedl, and Potere 2009). As an alternative, remote-sensing imagery can help significantly (Weng 2002; Yuan et al. 2005; Xiao et al. 2006). Landsat TM (Thematic

*Corresponding author. Email: liuxp3@mail.sysu.edu.cn

Mapper) and SPOT (Système Probatoire d'Observation de la Terre) satellites provide images with typically high spatial resolution. However, it is both labour intensive and time-consuming to explore regional or global areas due to their massive data volumes.

With coarser spatial resolution, desirable spectral resolution and temporal resolution, Moderate Resolution Imaging Spectroradiometer (MODIS) products can therefore meet the need for monitoring land-use and land-cover change (Justice et al. 1998; Thenkabail, Schull, and Turral 2005), especially at regional and even global scales. MODIS has supplied land-cover type products (e.g. MCD12Q1, 500 m; MCD12C1, 0.05°) annually since 2001 (Friedl et al. 2002, 2010), which have been considered as the most accurate among eight different global urban maps (Miyazaki, Iwao, and Shibasaki 2011). However, the image pixels of urban land in these products hardly change both quantitatively and spatially every year. This observation is unreasonable in fast-growing regions such as China. MODIS also provides researchers with surface reflectance products that can be classified into several land-cover types using various classification methods. For example, Gonçalves et al. (2005) used the MOD09A1 product for land-cover classification in Portugal. In this method, nevertheless, the problems of the same object with different spectra and different objects with similar spectra still remain unsolved. It is a difficult task to distinguish urban and bare lands simply based on spectral information of several bands from surface reflectance data, regardless of the classifier used.

In fact, to avoid the aforementioned difficulties, night-time light products from the Defense Meteorological Satellite Program's Operational Linescan System (DMSP-OLS) have also long been used successfully in studies of mapping urban land and suchlike (e.g. Imhoff et al. 1997; Elvidge et al. 2001; Lo 2002; Small, Pozzi, and Elvidge 2005). The data have to be intercalibrated first for multi-temporal analysis because OLS has no on-board calibration (Elvidge et al. 2009). However, no widely accepted intercalibration model exists up to now. In addition, data saturation (i.e. digital number values are invariant in urban cores) is another serious problem that significantly affects the accuracy of urban land mapping (Elvidge et al. 2007). What is worse, commonly used threshold-based methods for extraction not only overestimate the extent of urban land around megacities because of the blooming effect, but also omit underdeveloped cities (Henderson et al. 2003; Small, Pozzi, and Elvidge 2005). Fortunately, Lu et al. (2008) have proposed a human settlement index based on DMSP-OLS data and the normalized difference vegetation index (NDVI) to map human settlements in southeastern China. They found that NDVI data can be used to reduce the blooming effect and pixel saturation of night-time light products. A combined use of DMSP-OLS and NDVI data can provide better performance than when each method is used alone (Lu et al. 2008; Cao et al. 2009). Moreover, NDVI data are quite appealing and helpful for researchers to distinguish urban and bare lands (Lenney et al. 1996; Masek, Lindsay, and Goward 2000). Clearly, urban land extraction with multiple source data is feasible and useful (Schneider, Friedl, and Woodcock 2003; Ran et al. 2012). Thus, all three data sets, namely MODIS surface reflectance, MODIS NDVI, and DMSP-OLS data, are used to extract urban land in this study.

Since our study is only interested in extracting urban land from remote-sensing images, it can be regarded as one-class classification (Foody et al. 2006; Sanchez-Hernandez, Boyd, and Foody 2007). While traditional supervised classification methods are inefficient (Foody et al. 2006; Munoz-Mari, Bruzzone, and Camps-Valls 2007), support vector machine (SVM) has been commonly employed in one-class classification of remote-sensing images and has been found useful in recent years (Hermes et al. 1999; Foody et al. 2006; Munoz-Mari, Bruzzone, and Camps-Valls 2007; Sanchez-Hernandez, Boyd, and Foody 2007). For instance, Cao et al. (2009) proposed a SVM-based method to

extract urban areas of 25 Chinese cities by combining NDVI and DMSP-OLS data. Yang, He, and Du (2011) presented a stratified SVM-based method to map urban land of China. Pandey, Joshi, and Seto (2013) employed the SVM-based method to extract urban areas of India. However, SVM relies heavily on the choice of parameters and kernel, which often leads to a trial-and-error approach. In addition, the speed and size of SVM limit its applications in practice (Burges 1998; Mountrakis, Im, and Ogole 2011). Thus, devising a robust one-class classification method remains necessary in order to extract urban land more quickly, easily, and accurately.

Interestingly, Phillips, Dudík, and Schapire (2004) developed software (MAXENT), based on the maximum entropy model, to solve the one-class problems in ecological niche modelling. This model can conveniently offer the potential distribution of one or more given species according to presence-only data (Phillips, Dudík, and Schapire 2004; Phillips, Anderson, and Schapire 2006) since reliable absence data are difficult to obtain (Hirzel et al. 2002). Recently, MAXENT has been applied to one-class classification of remote-sensing images, the results of which proved to be superior of this novel method compared with one-class SVM (Li and Guo 2010). Accordingly, our study proposes a maximum entropy method to extract urban land by combining MODIS surface reflectance, NDVI, and DMSP-OLS data.

The main purpose of this study is to demonstrate the effectiveness of combining MAXENT, MODIS reflectance, NDVI, and DMSP-OLS data in one-class classification of remote-sensing images as well as to illustrate the unreliability of MODIS land-cover type product (MCD12Q1 in this study). The remainder of the article is organized as follows. Section 2 introduces the data used in this study. In Section 3, we describe the details of the proposed method. Section 4 presents the results from a case study. Finally, the discussion and conclusions are provided in Section 5.

2. Data and pre-processing

All the data used in this study were obtained freely through the Internet. The following are detailed information on the data (brief descriptions are listed in Table 1).

2.1. MODIS products

Available at http://reverb.echo.nasa.gov/reverb/, MODIS provides products with spatial resolution including 250 m, 500 m, and 1000 m. In this study, 500 m spatial resolution is more suitable when considering time and labour. Urban land extraction necessitates the use of the surface reflectance product (MOD09A1 for short) and vegetation index product (MOD13A1). Besides, the MCD12Q1 product was used for comparison, as shown in Section 4.2.

Table 1. Brief descriptions of the data used in this study.

Data set	Brief description	Acquisition time
MOD09A1	Surface reflectance product, 500 m, 8-day composite	From January to December for 2000, 2005, and 2010
MOD13A1	Vegetation index product, 500 m, 16-day composite	From January to December for 2000, 2005, and 2010
DMSP-OLS	Night-time lights product, 1000 m, yearly composite	2000, 2005, and 2010

2.1.1. MOD09A1

MODIS surface reflectance product has seven bands, namely bands 1 (620–670 nm), 2 (841–876 nm), 3 (459–479 nm), 4 (545–565 nm), 5 (1230–1250 nm), 6 (1628–1652 nm) and 7 (2105–2155 nm). This product is an estimate of the surface spectral reflectance for each band (Vermote and Kotchenova 2008). To achieve better performance, cloud screening was first performed based on the quality control flag of the images per scene each year. Next, we double checked the images to select the most cloud-free one. Each band of the images was separated as one independent environmental layer input for the implementation of MAXENT.

2.1.2. MOD13A1

The MODIS vegetation index product provides consistent spatial and temporal comparisons of global vegetation conditions, including two types of vegetation indices, namely NDVI and the enhanced vegetation index (EVI) (Solano et al. 2010). With a 16-day interval and 500 m spatial resolution, the NDVI data set from MOD13A1 product was selected as another environmental layer. To distinguish urban land and non-urban land thoroughly, a series of multi-temporal images were processed to a new $(\mathrm{NDVI})_{\max}$ image per calendar year through the maximum value composite procedure as follows (Lu et al. 2008):

$$(\mathrm{NDVI})_{\max} = \max\left[(\mathrm{NDVI})_1, (\mathrm{NDVI})_2, \ldots, (\mathrm{NDVI})_n\right], \tag{1}$$

where $(\mathrm{NDVI})_1$, $(\mathrm{NDVI})_2$, …, $(\mathrm{NDVI})_n$ are the multi-temporal NDVI values for each image within a 1-year period, each pixel is treated independently. This procedure can minimize the influence of clouds, water vapours, aerosols, and so on (Holben 1986).

2.1.3. MCD12Q1

The MODIS land-cover type product provides data for five different global land-cover classification systems such as the International Geosphere–Biosphere Programme (IGBP) global vegetation classification scheme and University of Maryland scheme. It has been produced annually since 2001 using a decision tree classification algorithm that is estimated with a database of high-quality land-cover training sites. We chose the commonly used IGBP scheme, which includes 17 land-cover types.

2.2. DMSP-OLS data

DMSP-OLS can detect the lights from human settlements such as cities, towns, and fires at night. In recent decades, the night-time lights product has been widely employed in mapping urban land. As a consequence, this product was naturally selected as the last environmental layer, which can avoid the intercalibration procedure. It has also been investigated that both the blooming effect and saturation phenomenon of the product can be reduced by using NDVI data (Lu et al. 2008; Cao et al. 2009).

2.3. Study area

The selected study area, China, has witnessed rapid urbanization since the implementation of reform and opening-up policy in 1978. Despite the economic development, a series of

severe problems arose such as arable land loss (Li and Yeh 2004; Liu, Wang, and Long 2010) and environmental damage (Chan and Yao 2008; Güneralp and Seto 2008; Pei et al. 2013). Consequently, analysis of urban land expansion in China during the past decade is an urgent and meaningful endeavour.

3. Methodology

In general, training samples of all land-cover types are necessary for image classification. In contrast, this study only required data of a positive class, namely urban land, which can be regarded as a species. In ecological niche modelling, a group of species tends to live in regions with suitable temperature, precipitation, elevation, soil type, and so on (Guo, Kelly, and Graham 2005). Similarly, the image pixels of urban land should have higher values in DMSP-OLS data and lower values in NDVI data. Accordingly, we are able to predict the potential distribution of the given species '*urban land*' in the geographical region of interest based on the MAXENT. The flowchart of the proposed method is presented in Figure 1.

3.1. *Maximum entropy model*

Entropy, a concept borrowed from thermodynamics, can measure how much 'choice' is involved in the selection of an event (Shannon 1948). Higher entropy of a distribution indicates that more choices are involved. First proposed by Jaynes (1957), the MAXENT is especially well suited for presence-only data sets (Phillips, Anderson, and Schapire 2006). The principle behind this concept is to model everything that is already known and assume nothing about that which is unknown (Berger, Pietra, and Pietra 1996).

Just let a finite set X denote the geographical region of interest, a number of random points $x_1, x_2,\ldots, x_m$ in X denote positive training samples, together with a set of features f_1, $f_2,\ldots, f_n$ denoting several constraints, which are the incomplete information about the target distribution. Our goal is to estimate the unknown probability distribution π over X. We need to construct a distribution $\hat{\pi}$ that approximates π. The empirical distribution can be denoted as follows (Phillips, Dudík, and Schapire 2004):

$$\tilde{\pi}(x) = \frac{|\{1 \le i \le m : x_i = x\}|}{m}, \tag{2}$$

where m is the number of positive training samples.

The empirical average of f_j is defined as:

$$\tilde{\pi}[f_j] = \frac{1}{m}\sum_{i=1}^{m} f_j(x_i), \quad \text{for each feature } f_j, \tag{3}$$

where each feature f_j assigns a real value $f_j(x)$ to each x in X.

We expect $\tilde{\pi}[f_j]$ to be close to its expectation $\pi[f_j]$ and attempt to find an approximation $\hat{\pi}$ that satisfies $\hat{\pi}[f_j] = \tilde{\pi}[f_j]$. There will be a number of distributions meeting these constraints, while the maximum entropy principle recommends that we should choose the one with maximum entropy from all of these distributions. The entropy of $\hat{\pi}$ is defined as:

$$H(\hat{\pi}) = -\sum_{x\in \mathrm{X}} \hat{\pi}(x)\ln\hat{\pi}(x), \tag{4}$$

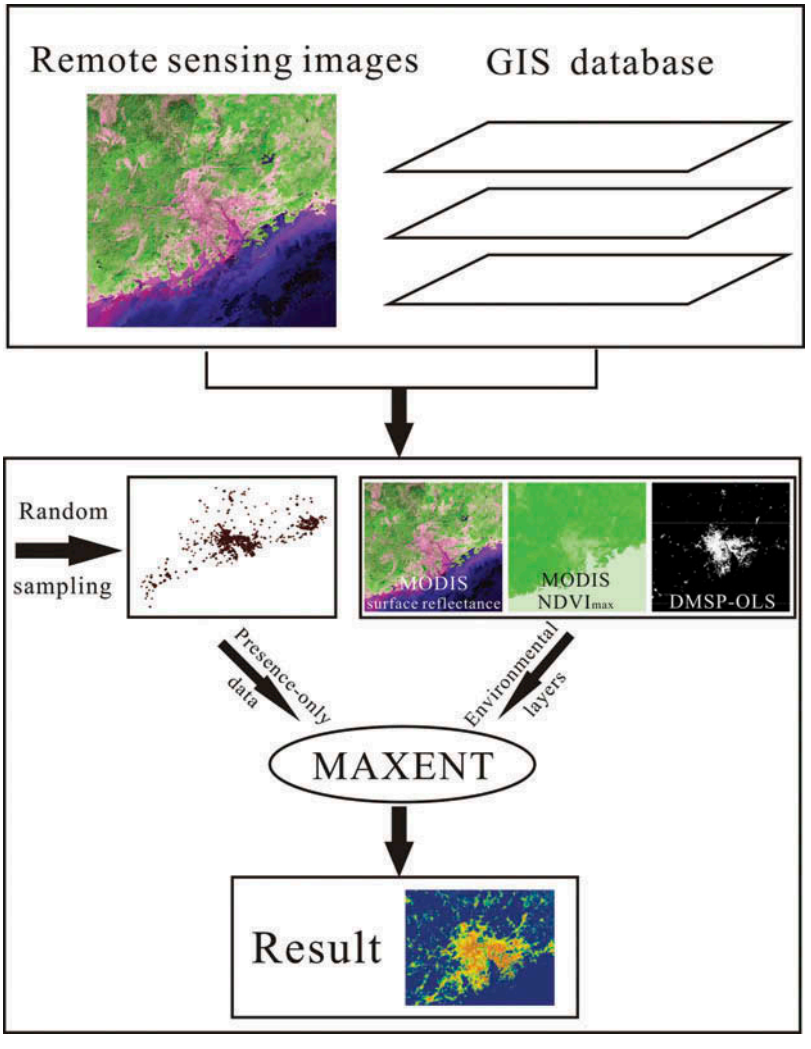

Figure 1. Flowchart of urban-land extraction based on maximum entropy model.

where ln is the natural logarithm.

More detailed information about the MAXENT can be seen in the works of Phillips, Dudík, and Schapire (2004) and Phillips, Anderson, and Schapire (2006).

3.2. *Implementation of MAXENT*

MAXENT is software developed by Phillips, Dudík, and Schapire (2004), which can be freely downloaded at http://www.cs.princeton.edu/~schapire/maxent/. This user-friendly software requires only two sets of data for running: georeferenced locations of presence-only training samples and several corresponding environmental variables of the whole study area (Phillips, Dudík, and Schapire 2004; Phillips, Anderson, and Schapire 2006). MAXENT is both time- and labour-saving because absence data are unnecessary. In this study, we randomly selected 2000 sample points of urban land and 1000 sample points of

non-urban land from MOD09A1 images per scene by visual interpretation, and then saved their x and y coordinates as a CSV file. Only 1000 presence samples were available for training, and the remaining 1000 presence and absence samples were available for threshold tuning (described in the next section).

All of the data mentioned in Section 2 were used as the environmental layer inputs after rescaling into the range [0, 1]. The logistic output format was chosen because it can achieve better performance compared with cumulative and raw output formats (Phillips and Dudík 2008). Moreover, we chose the default option 'auto features', which automatically determines the most suitable complexity based on the sample size of presence records (Merckx et al. 2011; Syfert, Smith, and Coomes 2013). The random test percentage was set as 25% (Young, Carter, and Evangelista 2011). Other user-specified parameters were set to their default values in accordance with related studies: regularization multiplier = 1, maximum iterations = 500, and convergence threshold = 10^{-5} (Li and Guo 2010; Guo et al. 2011). To obtain more reliable results, we ran MAXENT 15 times and then averaged the results from all models created.

3.3. *Threshold tuning*

After running MAXENT, only a probabilistic output will be given by the software. Taking Figure 2 (the Pearl River Delta, PRD region in 2000) as an example, the different colour of each pixel indicates different probability of being positive. As a consequence, a threshold is necessary for converting the probabilistic output to binary prediction. However, the difficulty in threshold selection is a major drawback of MAXENT. Finding the appropriate threshold automatically poses difficulty if binary images are needed (Phillips, Anderson, and Schapire 2006; Guo et al. 2011). Thus, the thresholds were determined through an empirical method in this study, that is to say, we tuned the thresholds within the range [0, 1] with a 0.01 step increment, and then chose the one that maximizes the accuracy calculated by both presence and absence samples. To reduce subjective errors as much as possible, this task was fulfilled by the same

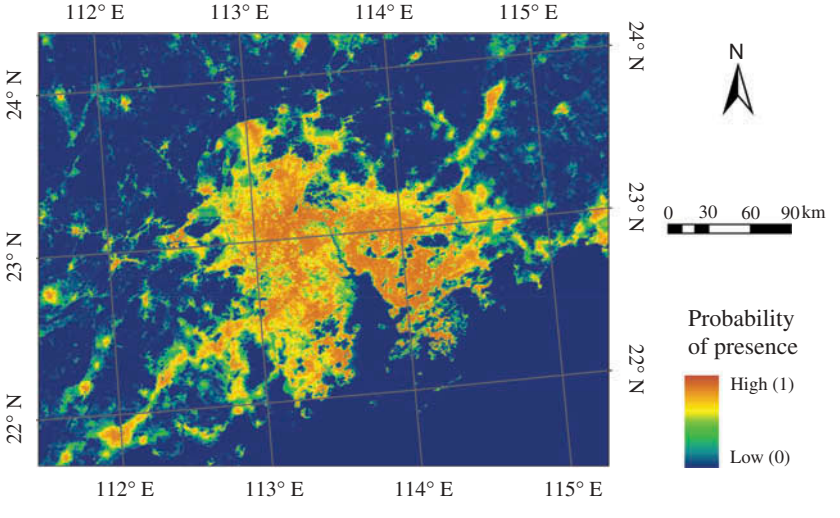

Figure 2. Original probabilistic output computed by MAXENT.

researcher with a consistent standard. It is interesting that the thresholds of a certain scene are quite similar each year. In addition, the thresholds are relatively lower in economically developed regions.

3.4. Validation methods

3.4.1. Internal validation

MAXENT provides two major internal validation methods, namely response curve and receiver operating characteristic (ROC) curve. The former illustrates how each environmental variable affects the MAXENT prediction, while the latter plots the sensitivity (true-positive rate) against specificity (false-positive rate) (Phillips, Anderson, and Schapire 2006). The larger the area under the ROC curve (AUC), the better will be the performance of the model. Since China is such a large area that up to 19 scenes of MODIS images should be involved for covering the whole country per year, we just selected a scene for analysis.

3.4.2. External validation

Given the finer spatial resolution (~30 m), the classified Landsat TM images were deemed to be validation references after being rescaled to the same resolution as the MODIS images. First, the probabilistic output was analysed by calculating the mean probability values of both urban and non-urban pixels in the classified Landsat TM images. Second, we compared the classification results of a scene using different combinations of the three data sets. Accuracy assessment was conducted by using a confusion matrix and kappa coefficient. We randomly selected 100 sample points of both urban land and non-urban land. Another 1000 sample points of both urban land and non-urban land each year were still required for validation of the final results. The potentially misleading high accuracies caused by the large amount of non-urban land in the whole country can be avoided by this random selection.

Third, the results of the proposed method were compared with those obtained from DMSP-OLS (the thresholds for binary classification were defined by comparing with the TM images [Henderson et al. 2003]) and MCD12Q1 data. Finally, studies have shown that urban growth correlates well with change in urban population and gross domestic product (GDP) (Elvidge et al. 2001; Liu et al. 2012). Therefore, we also conducted correlation analysis for further validation.

3.5. Monitoring urban expansion

Traditionally, researchers were apt to analyse land-use and land-cover change at national scale by administrative division. However, due to significant regional variations in such a large area like China, it is problematic to do so, no matter by province or by city. For instance, Guangdong Province is one of the most urbanized provinces in China, but the levels of urbanization and economic development vary from eastern to western regions. Moreover, the spatial distribution of urban land in the whole big country remains difficult to display distinctly. To address the aforementioned problems, we built a 25 km × 25 km square grid and then calculated the mean value (proportion) of urban land pixels within each grid per year. The spatiotemporal distribution of urban land can then be presented in a direct manner.

4. Results

4.1. Internal validation

The scene 'h28v06' in 2010 was selected for analysis. The corresponding response curves and ROC curve are shown in Figures 3 and 4, respectively. We can see from the response curves that urban areas are likely to occur in certain spectral conditions in NDVI and bands 1–7 of MOD09A1, and the probability of being positive increases with the DN value of DMSP-OLS data. In addition, an AUC value of 0.884 suggests that the model is well-performed (Phillips, Anderson, and Schapire 2006; Merckx et al. 2011). Since the response curves and ROC curves of different scenes are quite similar, the results of the proposed method are reliable.

4.2. External validation based on remote sensing data with fine spatial resolution

Taking Figure 2 as an example, the mean probability value of urban pixels in the corresponding classified TM images is 0.64, while the value of non-urban pixels is only 0.13. In addition, Figure 5 displays the comparison among extraction results using different combinations of the three data sets in PRD (scene 'h28v06') in 2005, and Table 2 lists the corresponding confusion matrices. Undoubtedly, the best results can be obtained when all three data sets were used (marked by the green circles in Figure 5). For example, distinguishing urban land and some rivers can be difficult without DMSP-OLS data (marked by the black ellipses), whereas the results extracted only using DMSP-OLS data were severely affected by the blooming effect and saturation.

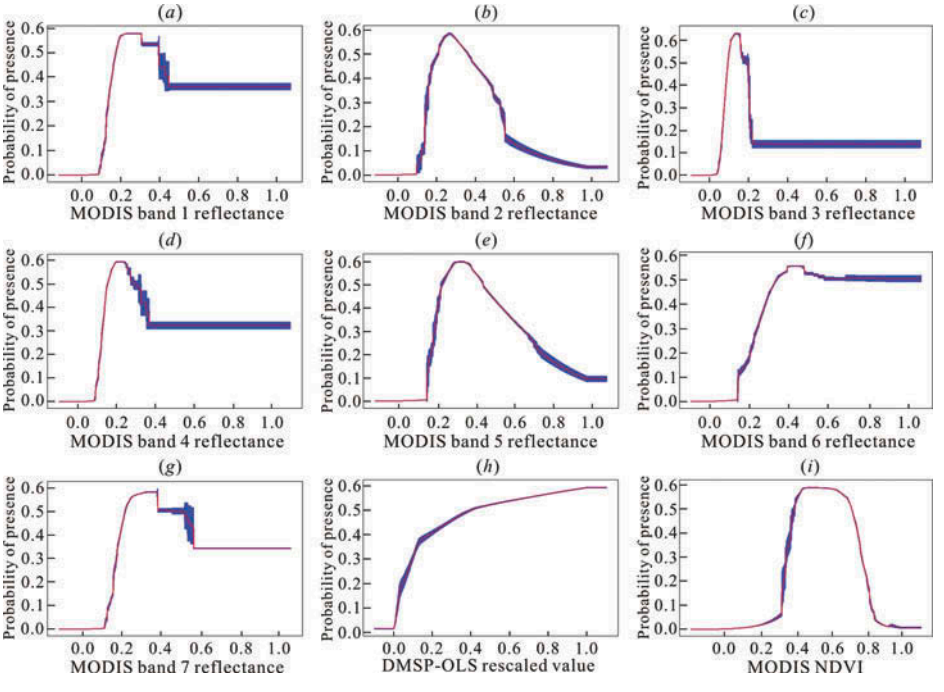

Figure 3. Response curves of the environmental layers. The curves show the mean response of the 15 replicate runs (purple) and the mean ±1 standard deviation (blue).

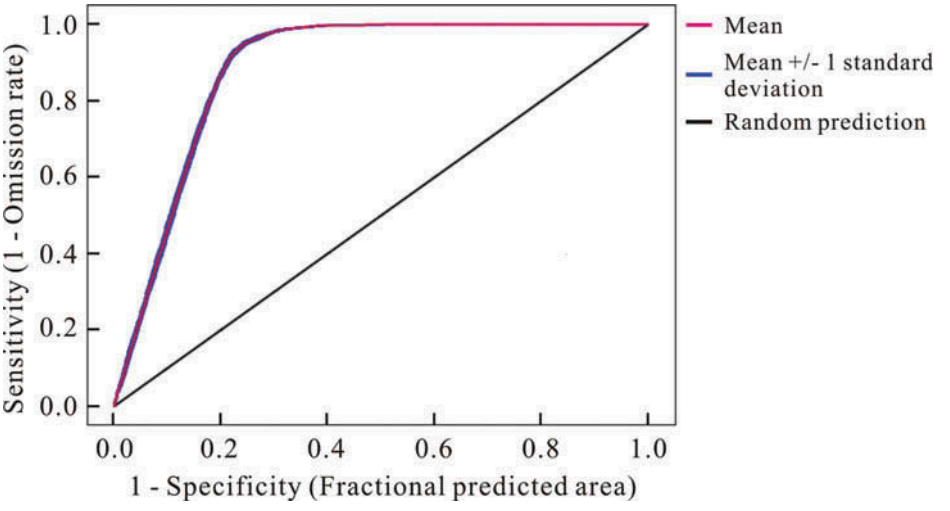

Figure 4. ROC curve of the scene 'h28v06' in 2010. The AUC value is 0.884.

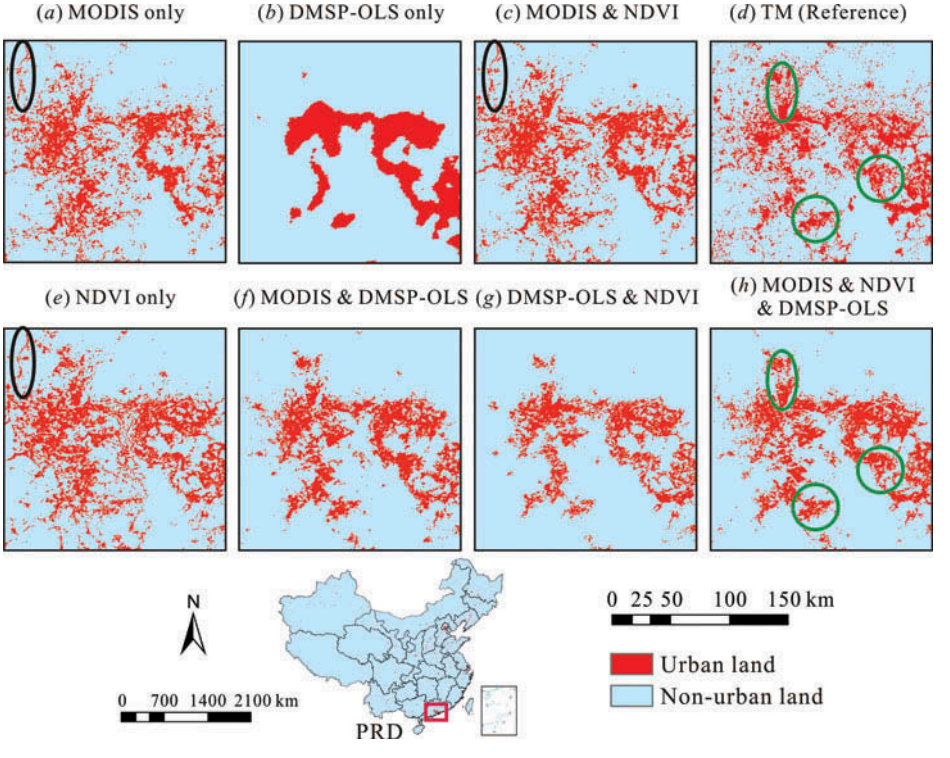

Figure 5. A comparison among extraction results using different combinations of the three data sets in the Pearl River Delta in 2005. The location map is shown at the bottom, and the longitude and latitude of the upper left corner of each box are 112.9° E, 23.6° N. The black and green ellipses highlight the differences among the results.

Table 2. Confusion matrix of extraction results using different combinations of the three data sets (with units of 500 m × 500 m pixels). The classified Landsat TM images were used as the reference data. 'M' stands for MODIS surface reflectance, 'N' for MODIS NDVI, and 'D' for DMSP-OLS data.

	M, N, D		M, N		M, D		N, D	
Results / Reference	Urban land	Non-urban land	Urban land	Non-urban land	Urban land	Non-urban land	Urban land	Non-urban land
Urban land	62	38	57	43	58	42	48	52
Non-urban land	0	100	2	98	0	100	2	98
Producer's accuracy	0.62	1.00	0.57	0.98	0.58	1.00	0.48	0.98
User's accuracy	1.00	0.72	0.97	0.70	1.00	0.70	0.96	0.65
Overall accuracy	0.81		0.78		0.79		0.73	
Kappa	0.62		0.55		0.58		0.46	

	M		N		D	
Results / Reference	Urban land	Non-urban land	Urban land	Non-urban land	Urban land	Non-urban land
Urban land	57	43	59	41	53	47
Non-urban land	1	99	4	96	0	100
Producer's accuracy	0.57	0.99	0.59	0.96	0.53	1.00
User's accuracy	0.98	0.70	0.94	0.70	1.00	0.68
Overall accuracy	0.78		0.78		0.77	
Kappa	0.56		0.55		0.53	

Therefore, by using a combination of the three data sets, the final urban land extraction results of China in 2000{C}, 2005{C}, and 2010{C} are presented in Figure 6. It is apparent that urban land of China was mainly distributed in several coastal areas such as the Yangtze River Delta region, PRD region, Beijing–Tianjin–Hebei metropolitan region, and followed by areas around several provincial capitals inland. With overall accuracies >0.75 (Table 3), the assessment indicates that the proposed method is rather effective compared with previous similar study (Liu et al. 2012) and MCD12Q1 data (Table 4). All the urban land extraction results are reliable enough for further analysis.

In addition, Figure 7 displays the comparison among extraction results obtained from the proposed method, Landsat TM images, and classification results of DMSP-OLS data by focusing on three major fast-growing cities in China. The comparison distinctly reveals the drawbacks of DMSP-OLS data as well as the success of the MAXENT-based method.

Finally, we can see from Figure 8 that the image pixels of urban land in MCD12Q1 data hardly change from 2001 to 2010 (only available since 2001). Meanwhile, the extraction results of the proposed method are comparable to the classified Landsat TM images. The spatiotemporal distribution patterns are rather similar between the latter two.

4.3. *External validation based on socioeconomic statistical data*

To further evaluate the performance of the MAXENT-based method, we also conducted correlation analysis between change in urban land by province and change in urban

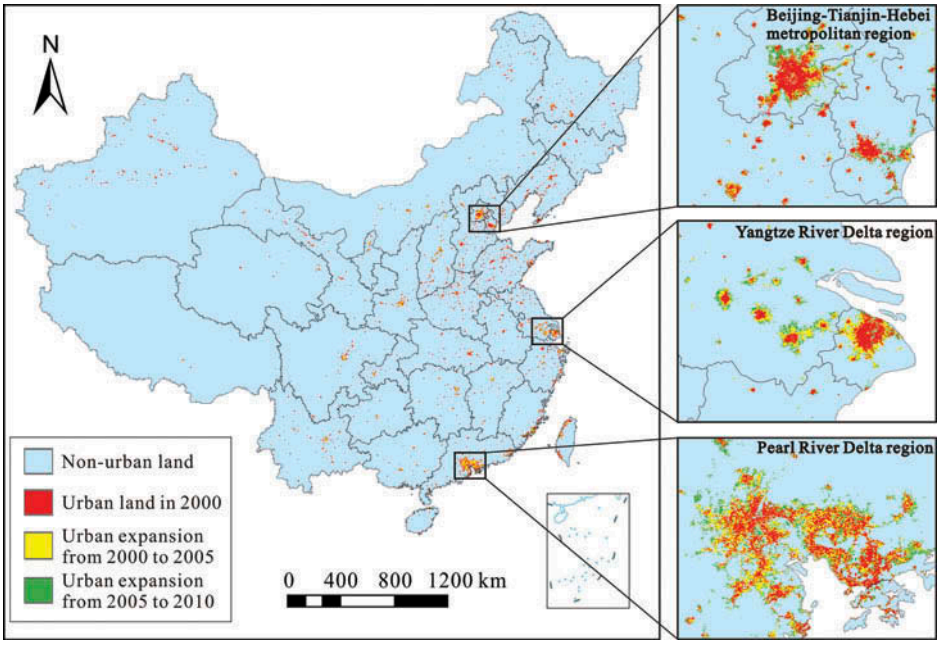

Figure 6. Urban land extraction results of China in 2000{C}, 2005{C}, and 2010{C}.

Table 3. Confusion matrix of final urban land extraction results (with units of 500 m × 500 m pixels). The classified Landsat TM images were used as the reference data.

	2000		2005		2010	
Results Reference	Urban land	Non-urban land	Urban land	Non-urban land	Urban land	Non-urban land
Urban land	533	5	518	5	529	7
Non-urban land	467	995	482	995	471	993
Producer's accuracy	0.991	0.681	0.990	0.674	0.987	0.678
User's accuracy	0.533	0.995	0.518	0.995	0.529	0.993
Overall accuracy	0.764		0.757		0.761	
Kappa	0.528		0.513		0.522	

Table 4. Confusion matrix of MCD12Q1 data (with units of 500 m × 500 m pixels). The classified Landsat TM images were used as the reference data.

	2001		2005		2010	
Results Reference	Urban land	Non-urban land	Urban land	Non-urban land	Urban land	Non-urban land
Urban land	457	2	489	3	504	6
Non-urban land	543	998	511	997	496	994
Producer's accuracy	0.996	0.648	0.994	0.661	0.988	0.667
User's accuracy	0.457	0.998	0.489	0.997	0.504	0.994
Overall accuracy	0.728		0.743		0.749	
Kappa	0.455		0.486		0.498	

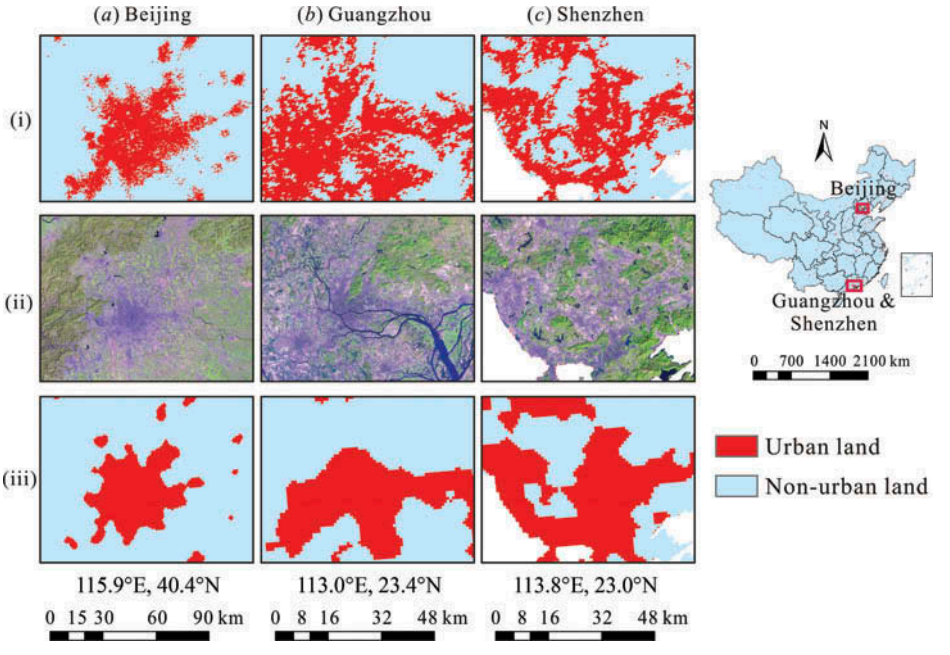

Figure 7. A comparison among (i) extraction results obtained from the MAXENT-based method, (ii) Landsat TM image, and (iii) classification results obtained from DMSP-OLS data in 2005. The location map is shown to the right, and the longitude and latitude of the upper left corner of each box are indicated at the bottom.

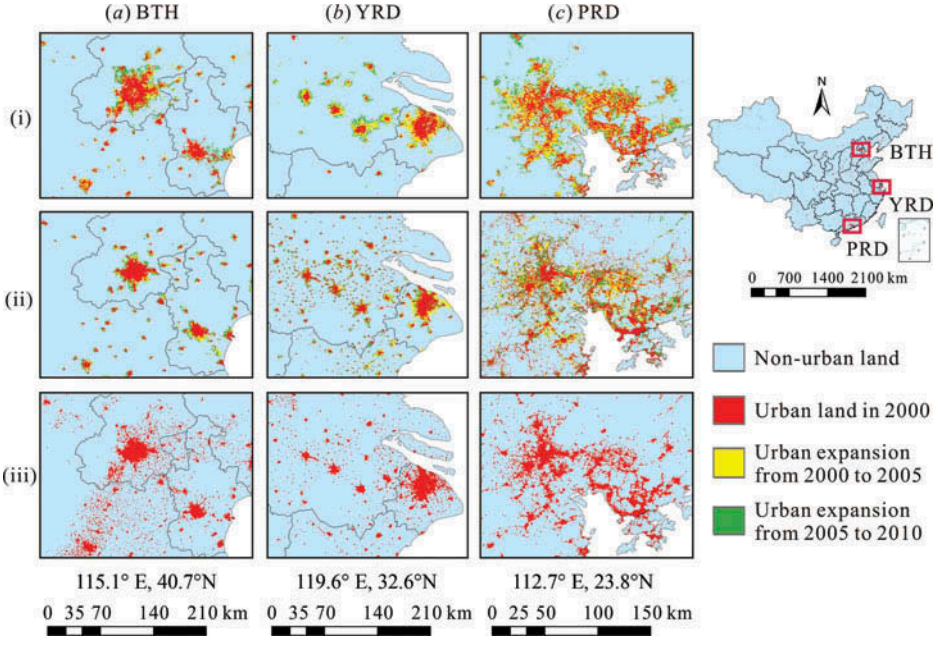

Figure 8. Urban expansion in (i) the MAXENT-based method, (ii) classified Landsat TM images, and (iii) MCD12Q1 data from 2000 to 2010. The location map is shown to the right, and the longitude and latitude of the upper left corner of each box are indicated at the bottom. 'BTH' stands for Beijing–Tianjin–Hebei metropolitan region, 'YRD' for Yangtze River Delta region, and 'PRD' for Pearl River Delta region.

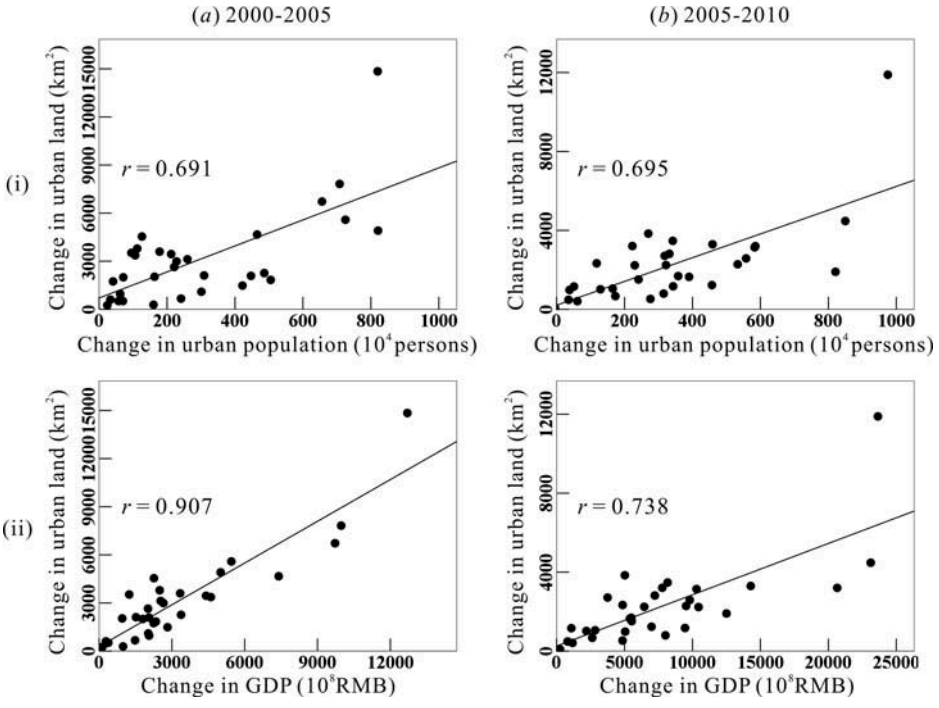

Figure 9. Correlation analysis between change in urban land and change in (i) urban population and (ii) GDP during (*a*) 2000{C}–2005{C} and (*b*) 2005{C}–2010{C}. *r* stands for correlation coefficient.

population, change in GDP, respectively. Change in urban population and change in GDP by province were calculated by referring to statistical data acquired from the National Bureau of Statistics of China in 2000{C}, 2005{C}, and 2010{C}. The results shown in Figure 9 suggest that the change in urban land correlates well with both change in urban population and GDP by province, with Pearson correlation coefficients around 0.70 (all correlations are significant at the 0.01 level).

4.4. Monitoring urban expansion in China

According to the final urban land extraction results, the urban area in China significantly increased from 27,406.55 km^2 in 2000 to 48,628.13 km^2 in 2005, and further to 63,434.21 km^2 in 2010, with growth rates of 77.43 and 30.45%, respectively. Figures 10–12 illustrate the spatio-temporal distribution of urban land. In 2000, highly urbanized regions were mainly distributed in several city cores around coastal areas, such as Beijing, Tianjin, Shanghai, Guangzhou, and Shenzhen. In addition, Dongguan, Qingdao, Xi'an and Suzhou, Chengdu, Dalian, etc. reached a higher level of urbanization in 2005 and 2010, respectively. We focused on three different fast-growing regions each year, clearly showing the urbanization process in metropolitan areas and their positive effects on neighbouring regions. For instance, the rapid urbanization of Guangzhou has spurred the development of city cores of Dongguan and Foshan.

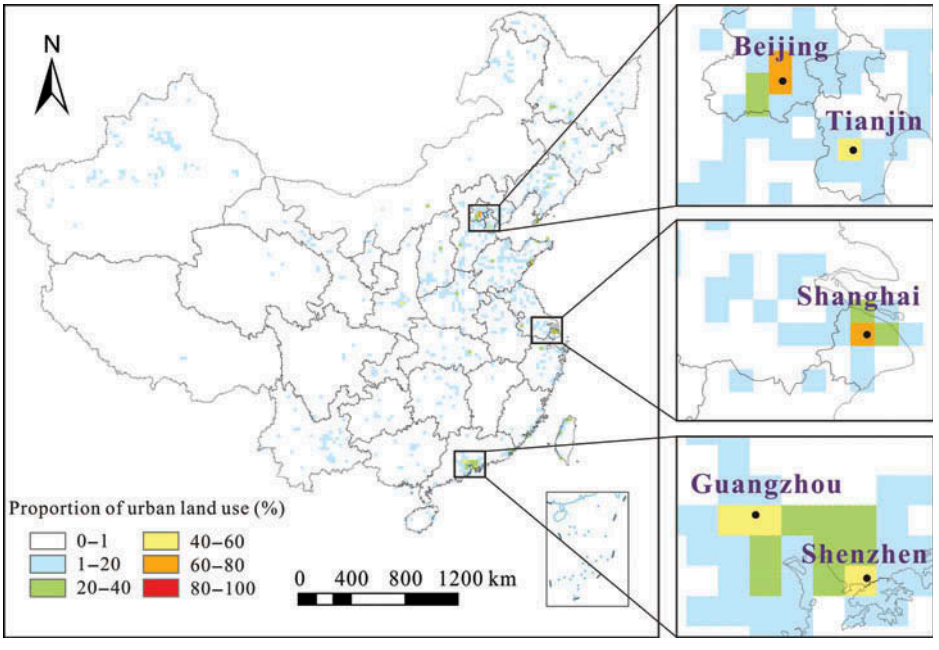

Figure 10. Spatial distribution of urban land in 2000.

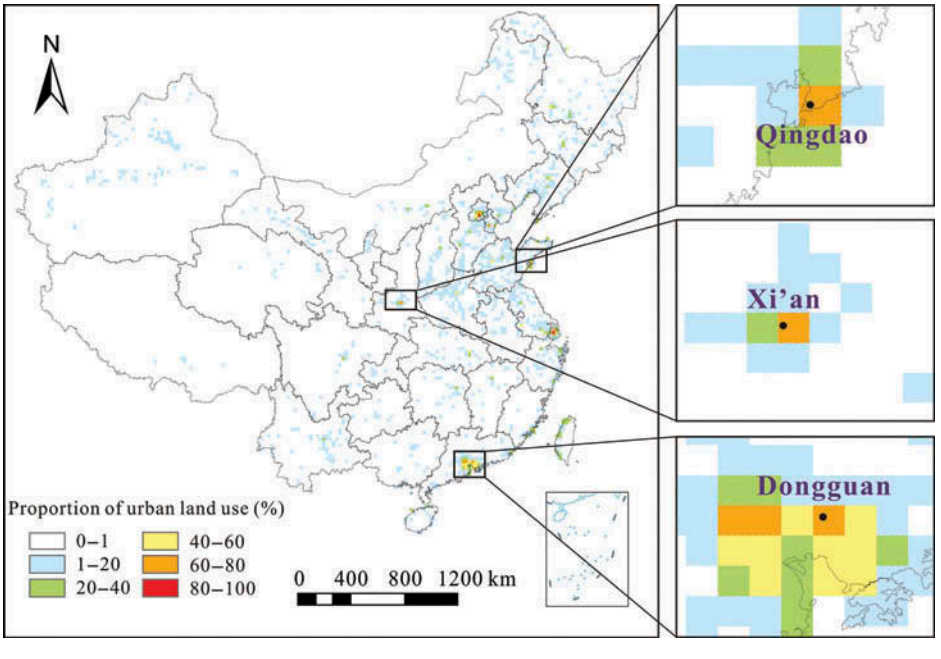

Figure 11. Spatial distribution of urban land in 2005.

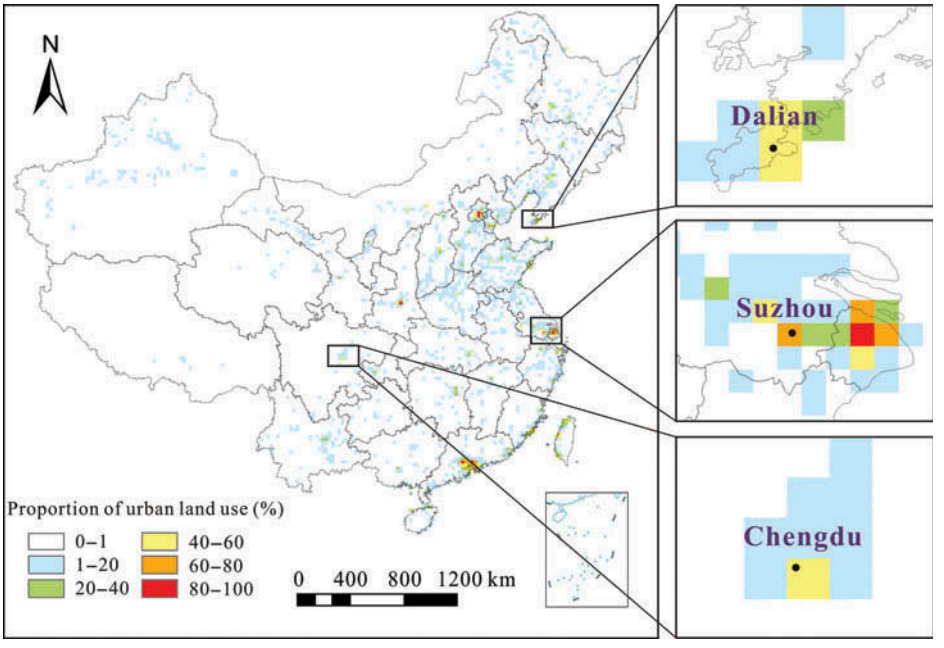

Figure 12. Spatial distribution of urban land in 2010.

5. Discussion and conclusions

It is often the case that researchers are only interested in extracting urban land from remote sensing images such as MODIS products. However, mere dependence on spectral information of several bands from surface reflectance data poses problems in applying traditional methods of remote sensing image classification. For instance, distinguishing urban and bare lands become difficult.

Moreover, traditional classification methods are inefficient because training samples of all land-cover types are necessary. Although SVM shows promise in one-class classification, this method relies strongly on the choice of parameters and kernel (Burges 1998; Mountrakis, Im, and Ogole 2011). In fact, it underperformed compared with MAXENT, a current cutting-edge classifier in ecological niche modelling, as stated in a previous study (Li and Guo 2010). One major advantage of MAXENT is that it only requires presence data for running, which can significantly save time and effort. But the application of MAXENT in remote sensing remains limited. Therefore, this study has developed a MAXENT-based method to extract urban land by combining MODIS surface reflectance, MODIS NDVI, and DMSP-OLS data, all of which can be freely downloaded via the Internet. Despite the limitations of DMSP-OLS (e.g. blooming effect [Imhoff et al. 1997]) and NDVI (e.g. difficulty in distinguishing urban land and other non-vegetation land-cover [Loveland et al. 2000]) data, a combination of them can provide more information to assist in the classification of MODIS images.

A multi-temporal case study of China demonstrates that this innovative method is rather effective for one-class classification of remote sensing images. It is especially promising in large-scale areas. Two internal validations indicate that the extraction results are reliable. Moreover, with overall accuracies >0.75, the results are comparable to the

classified Landsat TM images and are much better than the MODIS land-cover type product (MCD12Q1) with respect to both quantitative and visual comparisons. Since other global urban maps also have their own limitations (Global Rural–Urban Mapping Project severely overestimates city size for example) (Potere et al. 2009) and TM image classification spends massive time, effort, and money, the newly proposed method can be a feasible alternative for other periods and regions, especially at large scales.

Certainly, the MAXENT-based method still needs to be further tested and improved. For example, the probabilistic output can potentially be regarded as a development probability map, which is very useful in simulating and predicting urban growth. While some waterbodies were easily misclassified as urban land (Schneider, Friedl, and Potere 2009), they can be distinguished in our results. But the extraction results are fragmented to some extent. Besides, finding the optimal threshold automatically is difficult for MAXENT. Future efforts will be taken to overcome these drawbacks. Nevertheless, the newly created urban land data sets of China in 2000, 2005, and 2010 presented in this study might significantly help researchers and policy makers in various fields such as urban planning, urban ecology, simulation, and prediction of urban growth. Additionally, the proposed method can be further applied to other periods and regions ranging from regional to global scales.

Acknowledgements

We thank the editor and two anonymous referees for their useful comments and suggestions that greatly improved this paper.

Funding

This study was supported by the National Basic Research Programme of China (973 Programme) under Grant [number 2011CB707103]; the National Natural Science Foundation of China under Grant [number 41371376]; the Foundation for the Author of National Excellent Doctoral Dissertation of PR China under Grant [number 3149001]; and the National Science Fund for Excellent Young Scholars under Grant [number 41322009].

References

Balk, D. L., U. Deichmann, G. Yetman, F. Pozzi, S. I. Hay, and A. Nelson. 2006. "Determining Global Population Distribution: Methods, Applications and Data." *Advances in Parasitology* 62: 119–156. doi:10.1016/S0065-308X(05)62004-0.

Berger, A. L., V. J. D. Pietra, and S. A. D. Pietra. 1996. "A Maximum Entropy Approach to Natural Language Processing." *Computational Linguistics* 22 (1): 39–71.

Burges, C. J. 1998. "A Tutorial on Support Vector Machines for Pattern Recognition." *Data Mining and Knowledge Discovery* 2 (2): 121–167. doi:10.1023/A:1009715923555.

Cao, X., J. Chen, H. Imura, and O. Higashi. 2009. "A SVM-Based Method to Extract Urban Areas from DMSP-OLS and SPOT VGT Data." *Remote Sensing of Environment* 113 (10): 2205–2209. doi:10.1016/j.rse.2009.06.001.

Chan, C. K., and X. Yao. 2008. "Air Pollution in Mega Cities in China." *Atmospheric Environment* 42 (1): 1–42. doi:10.1016/j.atmosenv.2007.09.003.

Elvidge, C. D., P. Cinzano, D. Pettit, J. Arvesen, P. Sutton, C. Small, R. Nemani, T. Longcore, C. Rich, J. Safran, J. Weeks, and S. Ebener. 2007. "The Nightsat Mission Concept." *International Journal of Remote Sensing* 28 (12): 2645–2670. doi:10.1080/01431160600981525.

Elvidge, C. D., M. L. Imhoff, K. E. Baugh, V. R. Hobson, I. Nelson, J. Safran, J. B. Dietz, and B. T. Tuttle. 2001. "Night-Time Lights of the World: 1994–1995." *ISPRS Journal of Photogrammetry and Remote Sensing* 56 (2): 81–99. doi:10.1016/S0924-2716(01)00040-5.

Elvidge, C. D., D. Ziskin, K. E. Baugh, B. T. Tuttle, T. Ghosh, D. W. Pack, E. H. Erwin, and M. Zhizhin. 2009. "A Fifteen Year Record of Global Natural Gas Flaring Derived from Satellite Data." *Energies* 2 (3): 595–622. doi:10.3390/en20300595.

Foody, G. M., A. Mathur, C. Sanchez-Hernandez, and D. S. Boyd. 2006. "Training Set Size Requirements for the Classification of a Specific Class." *Remote Sensing of Environment* 104 (1): 1–14. doi:10.1016/j.rse.2006.03.004.

Friedl, M. A., D. K. Mciver, J. C. Hodges, X. Zhang, D. Muchoney, A. H. Strahler, C. E. Woodcock, S. Gopal, A. Schneider, A. Cooper, A. Baccini, F. Gao, and C. Schaaf. 2002. "Global Land Cover Mapping from MODIS: Algorithms and Early Results." *Remote Sensing of Environment* 83 (1–2): 287–302. doi:10.1016/S0034-4257(02)00078-0.

Friedl, M. A., D. Sulla-Menashe, B. Tan, A. Schneider, N. Ramankutty, A. Sibley, and X. Huang. 2010. "MODIS Collection 5 Global Land Cover: Algorithm Refinements and Characterization of New Datasets." *Remote Sensing of Environment* 114 (1): 168–182. doi:10.1016/j.rse.2009.08.016.

Gonçalves, P., H. Carrão, A. Pinheiro, and M. Caetano. 2005. "Land Cover Classification with Support Vector Machine Applied to MODIS Imagery". In *Proceedings of the 25th EARSeL Symposium*.

Grimm, N. B., S. H. Faeth, N. E. Golubiewski, C. L. Redman, J. Wu, X. Bai, and J. M. Briggs. 2008. "Global Change and the Ecology of Cities." *Science* 319 (5864): 756–760. doi:10.1126/science.1150195.

Güneralp, B., and K. C. Seto. 2008. "Environmental Impacts of Urban Growth from an Integrated Dynamic Perspective: A Case Study of Shenzhen, South China." *Global Environmental Change* 18 (4): 720–735. doi:10.1016/j.gloenvcha.2008.07.004.

Guo, Q., M. Kelly, and C. H. Graham. 2005. "Support Vector Machines for Predicting Distribution of Sudden Oak Death in California." *Ecological Modelling* 182 (1): 75–90. doi:10.1016/j.ecolmodel.2004.07.012.

Guo, Q., W. Li, Y. Liu, and D. Tong. 2011. "Predicting Potential Distributions of Geographic Events Using One-Class Data: Concepts and Methods." *International Journal of Geographical Information Science* 25 (10): 1697–1715. doi:10.1080/13658816.2010.546360.

Henderson, M., E. T. Yeh, P. Gong, C. Elvidge, and K. Baugh. 2003. "Validation of Urban Boundaries Derived from Global Night-Time Satellite Imagery." *International Journal of Remote Sensing* 24 (3): 595–609. doi:10.1080/01431160304982.

Hermes, L., D. Frieauff, J. Puzicha, and J. M. Buhmann. 1999. "Support Vector Machines for Land Usage Classification in Landsat TM Imagery". IEEE International Geoscience and Remote Sensing Symposium, Hamburg, June 28–July 2.

Hirzel, A., J. Hausser, D. Chessel, and N. Perrin. 2002. "Ecological-Niche Factor Analysis: How to Compute Habitat-Suitability Maps without Absence Data?" *Ecology* 83 (7): 2027–2036. doi:10.1890/0012-9658(2002)083[2027:ENFAHT]2.0.CO;2.

Holben, B. N. 1986. "Characteristics of Maximum-Value Composite Images from Temporal AVHRR Data." *International Journal of Remote Sensing* 7 (11): 1417–1434. doi:10.1080/01431168608948945.

Imhoff, M. L., W. T. Lawrence, D. C. Stutzer, and C. D. Elvidge. 1997. "A Technique for Using Composite DMSP/OLS "City Lights" Satellite Data to Map Urban Area." *Remote Sensing of Environment* 61 (3): 361–370. doi:10.1016/S0034-4257(97)00046-1.

Jaynes, E. T. 1957. "Information Theory and Statistical Mechanics." *Physical Review* 106 (4): 620–630. doi:10.1103/PhysRev.106.620.

Justice, C. O., E. Vermote, J. R. Townshend, R. Defries, D. P. Roy, D. K. Hall, V. V. Salomonson, J. L. Privette, G. Riggs, A. Strahler, W. Lucht, R. B. Myneni, Y. Knyazikhin, S. W. Running, R. R. Nemani, Z. Wan, A. R. Huete, W. Van Leeuwen, R. E. Wolfe, L. Giglio, J. Muller, P. Lewis, and M. J. Barnsley. 1998. "The Moderate Resolution Imaging Spectroradiometer (MODIS): Land Remote Sensing for Global Change Research." *IEEE Transactions on Geoscience and Remote Sensing* 36 (4): 1228–1249. doi:10.1109/36.701075.

Lenney, M. P., C. E. Woodcock, J. B. Collins, and H. Hamdi. 1996. "The Status of Agricultural Lands in Egypt: The Use of Multitemporal NDVI Features Derived from Landsat TM." *Remote Sensing of Environment* 56 (1): 8–20. doi:10.1016/0034-4257(95)00152-2.

Li, W., and Q. Guo. 2010. "A Maximum Entropy Approach to One-Class Classification of Remote Sensing Imagery." *International Journal of Remote Sensing* 31 (8): 2227–2235. doi:10.1080/01431161003702245.

Li, X., J. Lin, Y. Chen, X. Liu, and B. Ai. 2013. "Calibrating Cellular Automata Based on Landscape Metrics by Using Genetic Algorithms." *International Journal of Geographical Information Science* 27 (3): 594–613. doi:10.1080/13658816.2012.698391.

Li, X., and A. G. O. Yeh. 2004. "Analyzing Spatial Restructuring of Land Use Patterns in a Fast Growing Region Using Remote Sensing and GIS." *Landscape and Urban Planning* 69 (4): 335–354. doi:10.1016/j.landurbplan.2003.10.033.

Liu, Y., J. Wang, and H. Long. 2010. "Analysis of Arable Land Loss and Its Impact on Rural Sustainability in Southern Jiangsu Province of China." *Journal of Environmental Management* 91 (3): 646–653. doi:10.1016/j.jenvman.2009.09.028.

Liu, Z., C. He, Q. Zhang, Q. Huang, and Y. Yang. 2012. "Extracting the Dynamics of Urban Expansion in China Using DMSP-OLS Nighttime Light Data from 1992 to 2008." *Landscape and Urban Planning* 106 (1): 62–72. doi:10.1016/j.landurbplan.2012.02.013.

Lo, C. 2002. "Urban Indicators of China from Radiance-Calibrated Digital DMSP-OLS Nighttime Images." *Annals of the Association of American Geographers* 92 (2): 225–240. doi:10.1111/1467-8306.00288.

Loveland, T., B. Reed, J. Brown, D. Ohlen, Z. Zhu, L. Yang, and J. Merchant. 2000. "Development of a Global Land Cover Characteristics Database and IGBP Discover from 1 km AVHRR Data." *International Journal of Remote Sensing* 21 (6–7): 1303–1330. doi:10.1080/014311600210191.

Lu, D., H. Tian, G. Zhou, and H. Ge. 2008. "Regional Mapping of Human Settlements in Southeastern China with Multisensor Remotely Sensed Data." *Remote Sensing of Environment* 112 (9): 3668–3679. doi:10.1016/j.rse.2008.05.009.

Masek, J., F. Lindsay, and S. Goward. 2000. "Dynamics of Urban Growth in the Washington DC Metropolitan Area, 1973–1996, from Landsat Observations." *International Journal of Remote Sensing* 21 (18): 3473–3486. doi:10.1080/014311600750037507.

Merckx, B., M. Steyaert, A. Vanreusel, M. Vincx, and J. Vanaverbeke. 2011. "Null Models Reveal Preferential Sampling, Spatial Autocorrelation and Overfitting in Habitat Suitability Modelling." *Ecological Modelling* 222 (3): 588–597. doi:10.1016/j.ecolmodel.2010.11.016.

Miyazaki, H., K. Iwao, and R. Shibasaki. 2011. "Development of a New Ground Truth Database for Global Urban Area Mapping from a Gazetteer." *Remote Sensing* 3 (6): 1177–1187. doi:10.3390/rs3061177.

Mountrakis, G., J. Im, and C. Ogole. 2011. "Support Vector Machines in Remote Sensing: A Review." *ISPRS Journal of Photogrammetry and Remote Sensing* 66 (3): 247–259. doi:10.1016/j.isprsjprs.2010.11.001.

Munoz-Mari, J., L. Bruzzone, and G. Camps-Valls. 2007. "A Support Vector Domain Description Approach to Supervised Classification of Remote Sensing Images." *IEEE Transactions on Geoscience and Remote Sensing* 45 (8): 2683–2692. doi:10.1109/TGRS.2007.897425.

Pandey, B., P. Joshi, and K. C. Seto. 2013. "Monitoring Urbanization Dynamics in India Using DMSP/OLS Night Time Lights and SPOT-VGT Data." *International Journal of Applied Earth Observation and Geoinformation* 23: 49–61. doi:10.1016/j.jag.2012.11.005.

Pei, F., X. Li, X. Liu, S. Wang, and Z. He. 2013. "Assessing the Differences in Net Primary Productivity between Pre-and Post-Urban Land Development in China." *Agricultural and Forest Meteorology* 171–172: 174–186. doi:10.1016/j.agrformet.2012.12.003.

Phillips, S. J., R. P. Anderson, and R. E. Schapire. 2006. "Maximum Entropy Modeling of Species Geographic Distributions." *Ecological Modelling* 190 (3–4): 231–259. doi:10.1016/j.ecolmodel.2005.03.026.

Phillips, S. J., and M. Dudík. 2008. "Modeling of Species Distributions with Maxent: New Extensions and a Comprehensive Evaluation." *Ecography* 31 (2): 161–175. doi:10.1111/j.0906-7590.2008.5203.x.

Phillips, S. J., M. Dudík, and R. E. Schapire. 2004. "A Maximum Entropy Approach to Species Distribution Modeling." In *Proceedings of the twenty-first international conference on Machine learning*.

Potere, D., A. Schneider, S. Angel, and D. L. Civco. 2009. "Mapping Urban Areas on a Global Scale: Which of the Eight Maps Now Available Is More Accurate?" *International Journal of Remote Sensing* 30 (24): 6531–6558. doi:10.1080/01431160903121134.

Ran, Y., X. Li, L. Lu, and Z. Li. 2012. "Large-Scale Land Cover Mapping with the Integration of Multi-Source Information Based on the Dempster–Shafer Theory." *International Journal of Geographical Information Science* 26 (1): 169–191. doi:10.1080/13658816.2011.577745.

Sanchez-Hernandez, C., D. S. Boyd, and G. M. Foody. 2007. "One-Class Classification for Mapping a Specific Land-Cover Class: SVDD Classification of Fenland." *IEEE Transactions on Geoscience and Remote Sensing* 45 (4): 1061–1073. doi:10.1109/TGRS.2006.890414.

Schneider, A., M. A. Friedl, and D. Potere. 2009. "A New Map of Global Urban Extent from MODIS Satellite Data." *Environmental Research Letters* 4: 044003. doi:10.1088/1748-9326/4/4/044003.

Schneider, A., M. A. Friedl, and C. E. Woodcock. 2003. "Mapping Urban Areas by Fusing Multiple Sources of Coarse Resolution Remotely Sensed Data". IEEE International Geoscience and Remote Sensing Symposium, Toulouse, July 21–25.

Shannon, C. E. 1948. "A Mathematical Theory of Communication." *The Bell System Technical Journal* 27 (4): 623–656. doi:10.1002/j.1538-7305.1948.tb00917.x.

Small, C., F. Pozzi, and C. D. Elvidge. 2005. "Spatial Analysis of Global Urban Extent from DMSP-OLS Night Lights." *Remote Sensing of Environment* 96 (3–4): 277–291. doi:10.1016/j.rse.2005.02.002.

Solano, R., K. Didan, A. Jacobson, and A. Huete. 2010. *MODIS Vegetation Indices (MOD13) C5—User's Guide*, 1–38.

Stefanov, W. L., M. S. Ramsey, and P. R. Christensen. 2001. "Monitoring Urban Land Cover Change: An Expert System Approach to Land Cover Classification of Semiarid to Arid Urban Centers." *Remote Sensing of Environment* 77 (2): 173–185. doi:10.1016/S0034-4257(01)00204-8.

Syfert, M. M., M. J. Smith, and D. A. Coomes. 2013. "The Effects of Sampling Bias and Model Complexity on the Predictive Performance of Maxent Species Distribution Models." *PLoS ONE* 8 (2): e55158. doi:10.1371/journal.pone.0055158.

Thenkabail, P. S., M. Schull, and H. Turral. 2005. "Ganges and Indus River Basin Land Use/Land Cover (LULC) and Irrigated Area Mapping Using Continuous Streams of MODIS Data." *Remote Sensing of Environment* 95 (3): 317–341. doi:10.1016/j.rse.2004.12.018.

Vermote, E., and S. Kotchenova. 2008. *MOD09 (Surface Reflectance) User's Guide*, 1–29.

Weng, Q. 2002. "Land Use Change Analysis in the Zhujiang Delta of China Using Satellite Remote Sensing, GIS and Stochastic Modelling." *Journal of Environmental Management* 64 (3): 273–284. doi:10.1006/jema.2001.0509.

Xiao, J., Y. Shen, J. Ge, R. Tateishi, C. Tang, Y. Liang, and Z. Huang. 2006. "Evaluating Urban Expansion and Land Use Change in Shijiazhuang, China, by Using GIS and Remote Sensing." *Landscape and Urban Planning* 75 (1–2): 69–80. doi:10.1016/j.landurbplan.2004.12.005.

Yang, Y., C. He, and S. Du. 2011. "Improving the Support Vector Machine-Based Method to Map Urban Land of China Using DMSP/OLS and SPOT VGT Data." IEEE International Geoscience and Remote Sensing Symposium, Vancouver, July 24–29.

Young, N., L. Carter, and P. Evangelista. 2011. *A Maxent Model V3.3.3e Tutorial (ArcGIS V10)*, 1–30.

Yuan, F., K. E. Sawaya, B. C. Loeffelholz, and M. E. Bauer. 2005. "Land Cover Classification and Change Analysis of the Twin Cities (Minnesota) Metropolitan Area by Multitemporal Landsat Remote Sensing." *Remote Sensing of Environment* 98 (2–3): 317–328. doi:10.1016/j.rse.2005.08.006.